JOURNAL OF Materials CHEMISTRY

Excitation energy transfer and spatial exciton confinement in polyfluorene blends for application in light-emitting diodes

Ana Charas,[a,b] **Jorge Morgado,***[a,b] **J. M. G. Martinho,**[a] **A. Fedorov,**[a] **Luis Alcácer**[a,b] **and Franco Cacialli**[c,d]

[a]*Departamento de Engenharia Química, Instituto Superior Técnico, Avenida Rovisco Pais, P-1049-001 Lisboa, Portugal. E-mail: jmorgado@gcsi.ist.utl.pt*
[b]*Instituto de Telecomunicações, Avenida Rovisco Pais, P-1049-001 Lisboa, Portugal*
[c]*Cavendish Laboratory, Madingley Road, Cambridge, UK CB3 0HE*
[d]*Department of Physics and Astronomy, University College London, Gower Street, London, UK WC1E 6BT*

Received 24th June 2002, Accepted 24th September 2002
First published as an Advance Article on the web 23rd October 2002

We present picosecond time-resolved studies of thin films of two polyfluorene blends, combining a relatively high energy-gap poly(9,9-dioctylfluorene), PFO, and a polyfluorene derivative with a smaller gap. These studies show both efficient energy transfer from the donor to the acceptor, as well as spatial confinement of the excitons in the acceptor polymers. The optoelectronic characteristics of light-emitting diodes fabricated with such blends reflect the contribution of these two processes. The electroluminescence is almost exclusively from the acceptor polyfluorenes and we observe a significant improvement of the electroluminescence efficiency of the light-emitting diodes fabricated with such blends in comparison to those based on neat films of the polyfluorenes.

Introduction

Polymer blends have been used in the fabrication of optoelectronic devices, such as light-emitting diodes (LEDs) and photovoltaic cells. Depending on their relative frontier energy levels (highest occupied molecular orbital, HOMO, and lowest unoccupied molecular orbital, LUMO), photo-induced charge transfer or excitation energy transfer may become the predominant process.[1] While the first process is adequate for photovoltaic applications,[2,3] the second one is appropriate for LEDs.[4] The reasoning behind the use of polymer blends for LED fabrication lies in the possibility of separately controlling charge injection, charge transport, and light-emission processes. In addition there may be a separation of the emitting polymer chains within a matrix, which leads to an increase in their quantum yields of emission. This has been shown, in particular, when the polymer host is inert, from the point of view of charge transport and luminescence, as is the case with polystyrene.[5,6] The best advantages are, however, when the polymeric components play an active role in the charge transport and/or in the luminescence processes. The improvements in the electroluminescence, EL, efficiency of LEDs upon use of blends, result from an increase in the photoluminescence, PL, efficiency, as mentioned above, due to a dilution of the chromophores,[7] reducing the formation of low emissive interchain states,[6,8] such as aggregates or excimers. The improvement in charge injection and transport[9–11] efficient energy transfer, exciton confinement,[12,13] and combinations[14–17] have been held responsible for the EL efficiency increase upon use of blends in LEDs. The optimum blend should combine complementary charge transport, with the hole transporting component having no or negligible hole-injection barrier and similarly for the electron injection barrier into the electron-transporting material, with efficient energy transfer from the higher to the lower energy gap component and with spatial confinement of the excitons within the acceptor chains. The blends' tendency for phase separation, which can be accelerated by contact with non-solvents, for instance during LED fabrication,[18] enriches their physics. Although the use of polymer blends in LED fabrication has been very common, as mentioned above, the characterization of the excitation energy transfer[19–22] and exciton confinement[13] processes in such polymer blends is not so abundant. The use of time-resolved spectroscopy can be particularly useful to elucidate the importance of these processes in the photophysics of the blends.

Here, we report on the use of polyfluorene blends for the fabrication of LEDs and the characterization of these blends by picosecond time-resolved photoluminescence studies. Poly(9,9-dioctylfluorene), PFO, was chosen as the host polymer, due to a combination of high solid state PL efficiency (about 60%), good hole-transport properties and a blue emission spectrum overlapping with the absorption spectra of the two guest polyfluorene alternating copolymers, poly [9,9-bis(2′-ethylhexyl)fluoren-2,7-diyl-*alt*-2,2′:5′2″-terthiophene-5,5″-diyl], PF3T, and poly[9,9-bis(2′-ethylhexyl)fluoren-2,7-diyl-*alt*-*S*,*S*-dioxothiophene-2,5-diyl], PFTSO2[23] (see Fig. 1). The reason for the preparation of these blends lies in the observation of the

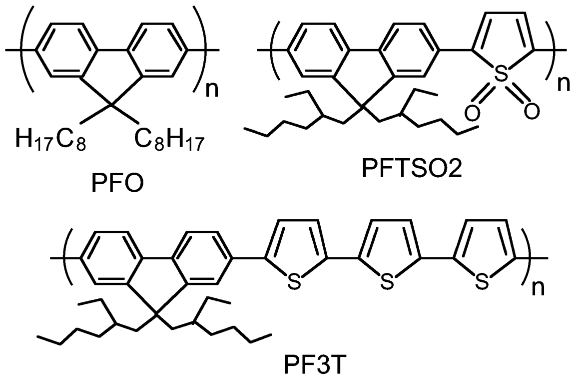

Fig. 1 Structure of the host polymer, PFO, and PF3T and PFTSO2 guest copolymers.

DOI: 10.1039/b206040j

Table 1 Optical and electrochemical properties of the copolymers PF3T and PFTSO2. Typical EL external quantum efficiencies and maximum luminance values obtained for single layer ITO/copolymer/Ca LEDs are also shown

Polymer	λ_{em}^{max}(film)/nm	η_{PL} (%) Soln (C_6H_{12})	 Film	E_{ox}^{onset}/V	E_{red}^{onset}/V	η_{EL} (%)	L_{max}/cd m^{-2}
PF3T	567, 609[a]	53	8.1	1.00	−1.58	4.4×10^{-3}	38
PFTSO2	615	19	0.5	1.23	−1.45	2.2×10^{-4}	0.2

[a] Two peaks.

strong reduction in PL efficiency of these two copolymers on going from solution to the solid state, which is severely detrimental for LED applications, when the neat copolymers are used as emissive layers.

Results and discussion

Table 1 summarizes the properties of PF3T and PFTSO2. The solid state PL efficiency of PF3T is higher than that of PFTSO2. As shown in Table 1, there is a strong PL reduction on going from dilute solution to solid state.

Fig. 2 compares the frontier energy levels of PFO[24] with those of PF3T and PFTSO2 estimated from the cyclic voltammetry data.[25] For the ITO work function we have considered a typical value of 4.8 eV, and for the PEDOT–PSS [poly(3,4-ethylene dioxythiophene) doped with poly(styrene sulfonic acid)] hole-injection layer the work function value was taken from ref. 26. Fig. 2 gives evidence of the necessary energy levels for energy transfer to be favored over charge separation. Note that, in addition to a good spectral overlap between donor's emission and acceptor's absorption spectra, the energy levels of the HOMO and LUMO of the acceptor should be within the HOMO–LUMO gap of the donor, in order to favor energy transfer over charge separation, as shown by Halls *et al.*[1] According to Fig. 2, the copolymer guests can act as both hole and electron trapping sites, favoring direct recombination within their chains. Furthermore, the hole and electron injection barriers are expected to be reduced if charge can be effectively injected directly into the guest domains, though, in view of its lower concentration, we anticipate that this might be an inefficient process.

Fig. 3 shows good spectral overlap of PFO emission (PL spectrum obtained for a solid film upon excitation at 395 nm) with the absorption spectra of PF3T and PFTSO2. In Fig. 3 we also compare the PL spectra of the blends, obtained upon excitation using a wavelength close to the maximum PFO absorption (400 nm), with the PL spectra of the neat guest copolymers both in dilute solution and as solid films.

In the case of the PFO–PF3T blends we find that there is a small PFO contribution to the total emission, and that the PF3T component of the total spectrum is similar to the PL spectrum of PF3T in dilute solution. The fact that the PF3T PL spectrum when in solution or in the blend is blue-shifted in relation to the spectrum of the solid film of neat PF3T, emphasizes the role played by the intermolecular (interchain) interactions and packing in the solid state. The PFO contribution to the total emission of PFO–PFTSO2 blends is larger than that found in PFO–PF3T blends. Note that, at 400 nm both components of the blends absorb, but since PFO is in a larger proportion, 95% by weight, we expect excitation photons to be mainly absorbed by PFO and direct excitation of PFTSO2 or PF3T to be very small.

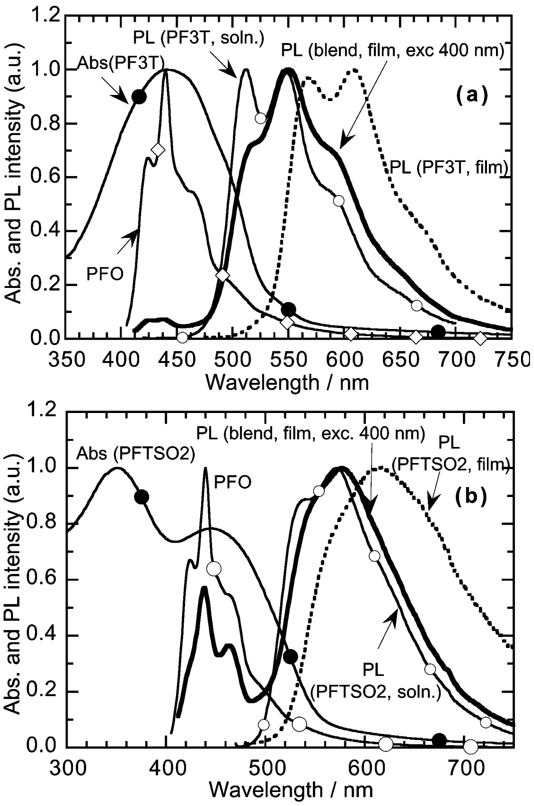

Fig. 3 Optical absorption spectra of PF3T (a) and PFTSO2 (b) and PL spectra of PFO, evidencing the good spectral overlap, which is required for an efficient long range energy transfer by the Förster mechanism. Also shown are the PL spectra of neat PF3T and PFTSO2, as thin films and in dilute cyclohexane solution, and of thin films of the blends.

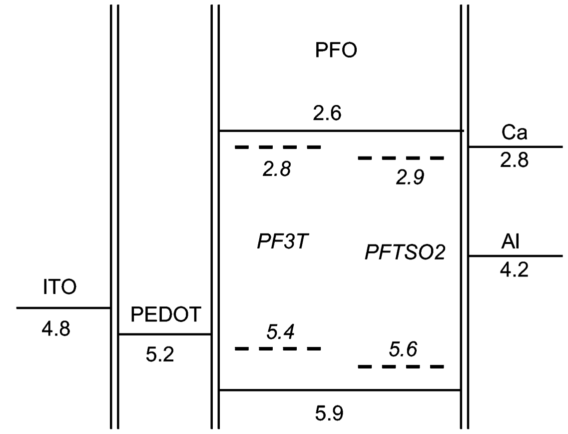

Fig. 2 Energy levels (eV) of the frontier orbitals.

Fig. 4 and 5 compare the fluorescence decay for the neat components, PF3T and PFTSO2, and their blends with PFO, obtained upon excitation at 340 nm. As mentioned above, photons impinging on the blends are mainly absorbed by PFO, because of its higher concentration.

The decay curves of the fluorescence intensity, $I_{PL}(t)$, were fitted according to the expression

$$I_{PL}(t) = \sum_{i=1}^{n} a_i \exp(-t/\tau_i)$$

For the blends we obtained $a_1 = -0.37$, $\tau_1 = 0.017$ ns; $a_2 = 0.80$,

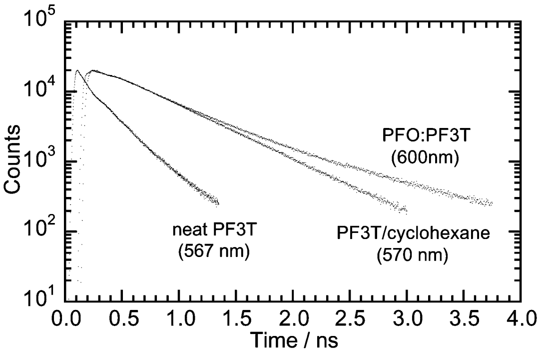

Fig. 4 Comparison of the fluorescence decay of the PFO–PF3T blend with that of the PF3T neat film and of the dilute solution of PF3T in cyclohexane, with detection at the wavelengths indicated.

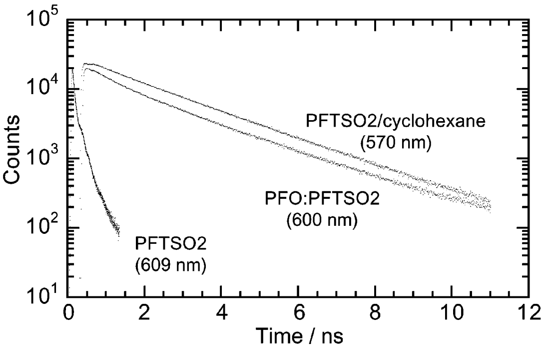

Fig. 5 Comparison of the fluorescence decay of the PFO–PFTSO2 blend with that of the PFTSO2 neat film and of the dilute solution of PFTSO2 in cyclohexane, with detection at the wavelengths indicated.

τ_2 = 0.436 ns; a_3 = 0.20, τ_3 = 1.099 ns; χ^2 = 1.059, for PFO–PF3T, and a_1 = −0.45, τ_1 = 0.030 ns; a_2 = 0.23, τ_2 = 2.977 ns; a_3 = 0.46, τ_3 = 1.572 ns; a_4 = 0.31, τ_4 = 0.345 ns; χ^2 = 1.066, for PFO–PFTSO2. The pre-exponential factors were normalized to a unitary value of the positive amplitudes. The results of the fitting of the fluorescence decay of the acceptor copolymers in dilute cyclohexane solutions, shown in Fig. 4 and 5, are a_1 = 0.57, τ_1 = 0.471 ns; a_2 = 0.43, τ_2 = 0.633 ns; χ^2 = 1.109, for PF3T, and a_1 = 0.69, τ_1 = 2.308 ns; a_2 = 0.16, τ_2 = 0.877 ns; a_3 = 0.15, τ_3 = 0.062 ns; χ^2 = 1.204, for PFTSO2.

The fluorescence decay of films of the blends shows, first of all, the presence of a negative component ("rise time"), which indicates an increase in the population of the excited state due to energy transfer from PFO to the guest copolymers. Aside from this rise time, the fluorescence decay is multi exponential as observed for the dilute cyclohexane solutions of the guest copolymers. A detailed report on the photophysics of the guest copolymers will be published elsewhere.

Though not shown, we observed that the decay of PFO fluorescence in the blends is much faster than in films of neat PFO, which is also in agreement with the existence of an energy transfer to the guest copolymers. As shown in Fig. 4 and 5, the fluorescence decay of the acceptor polymers in the blends is similar to that of the pure copolymers in dilute solution, and much slower than the fluorescence decay of films of the pure acceptor copolymers.

These time-resolved studies show that the dynamics of the excited states of the guest copolymers in the blends are similar to those in dilute solution. This indicates that the excitons are spatially confined to the guest copolymer chains.

The optoelectronic properties of the devices are not significantly altered when the guest copolymer is changed, with the maximum luminance reaching values of about 1500 cd m^{-2} at 10 V. A slightly smaller light-onset voltage is observed for devices based on the PFO–PF3T blend, in spite of the slightly thicker emissive layer.

Table 2 EL external quantum efficiencies of the various device structures fabricated with the PFO-based blends

Device structure	Max η_{EL}(%) PFO–PF3T	Max η_{EL}(%) PFO–PFTSO2
ITO/···/Al	0.035	0.015
ITO/PEDOT/···/Al	0.09	0.08
ITO/PEDOT/···/PBD/Al	0.20	0.21
ITO/PEDOT/···/Ca	0.22	0.14
ITO/PEDOT/neat acceptors/Ca	0.03	9×10^{-4}

Single-layer ITO/copolymer/Ca LEDs based on neat PF3T and PFTSO2 exhibit modest EL efficiency and maximum luminance, as shown in Table 1, which are attributed to a combination of low PL efficiency and charge transport limitations. Upon insertion of a hole-injection layer of PEDOT, the EL efficiency increases (as shown in Table 2), and the maximum luminance increases from 0.2 cd m^{-2} to about 5.3 cd m^{-2}, in the case of PFTSO2, though it decreases from 38 cd m^{-2} to 21 cd m^{-2}, in the case of PF3T. The optoelectronic characteristics of the ITO/PEDOT/neat copolymer/Ca devices are improved upon dispersion of the acceptor copolymers in PFO. Namely, there is a significant improvement in EL efficiency and luminance. The EL efficiency increase is about 9 times for PF3T and about 150 times for PFTSO2, as shown in Table 2. It is also worth mentioning that the light-onset voltage is reduced from 6 V to 4 V and from 16 V to 5–5.5 V for PFO–PF3T and PFO–PFTSO2 based devices, respectively (see Fig. 6 and 7).

Based on the frontier energy levels (see Fig. 2), it is expected that both holes and electrons should be trapped in the guest copolymers. However, we find that the current density of ITO/PEDOT/PFO (80 nm thick)/Al devices is only slightly higher than those of ITO/PEDOT/blend/Al LEDs (Fig. 6 and 7) while the light-onset voltage is similar. Therefore, the influence of the guest copolymers on the charge injection and transport in the blends, compared to neat PFO based LEDs, is small. The effect of charge trapping at the guest copolymer sites is, however, particularly evident when comparing the PL spectra of the blends (Fig. 3) with the EL spectra of their LEDs, shown in Fig. 8. In fact we observe that the PFO contribution to the EL emission is smaller than for the PL, particularly in the case of the PFO–PFTSO2 blend. This is attributed to direct electron-hole capture within the guest copolymer chains, since, according to Fig. 2, both electron and hole transfer to the guest

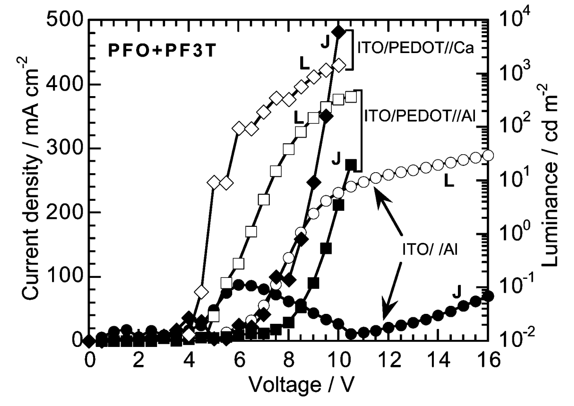

Fig. 6 Current density (J, filled symbols) and luminance (L, open symbols) as a function of the applied voltage, for LEDs based on PFO–PF3T (95 nm thick).

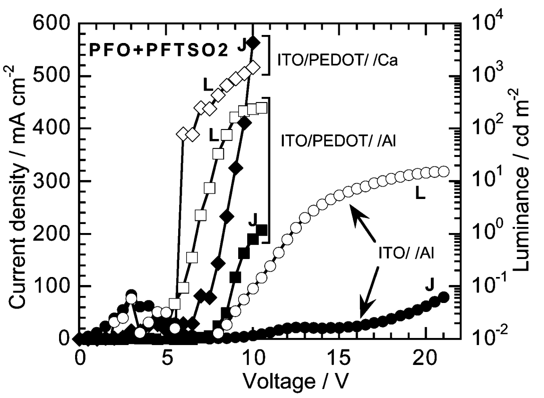

Fig. 7 Current density (J, filled symbols) and luminance (L, open symbols) as a function of the applied voltage, for LEDs based on PFO–PFTSO2 (80 nm thick).

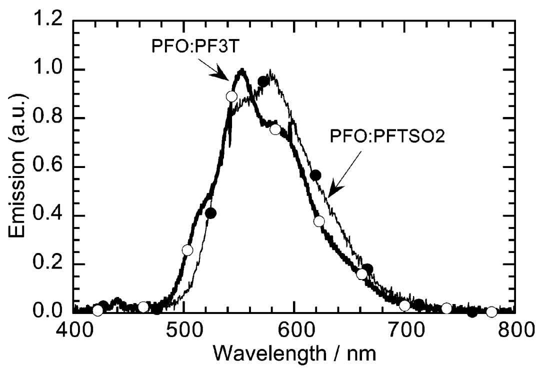

Fig. 8 Electroluminescence spectra for the blend-based LEDs.

copolymers, in addition to exciton transfer from the host PFO, are possible.

The improvement of the EL efficiency upon blending PF3T or PFTSO2 with PFO, is attributed to a combination of an efficient energy transfer process and an increase in the quantum yield. As we have discussed above, the time-resolved studies show that, upon blending, we recover a situation similar to a dilute solution from the excited state dynamics point of view. This is equivalent to spatial confinement of the excitons within the guest copolymer chains, in spite of being embedded in the PFO matrix. This leads, in turn, to an improvement in the emission quantum yield, approaching that of the solution situation. Therefore, we should expect that the PL efficiency of the copolymer guests in the blend should be comparable to their values in solution. Due to this exciton confinement within the acceptor copolymer chains, there will be also a large reduction of their migration to quenching sites in comparison with neat films. In addition to this effect, the increase in EL efficiency may also reflect the improvement of charge transport/balance within the device, as PFO is known as a good hole transporting material.[27] In fact, in the case of PFTSO2, the current increases by a factor of about 50 at 1.25 MV cm^{-1} in the same device structure when the blend is used. This indicates that, particularly in this case, charge transport and/or balance may be a limiting factor for the low EL efficiency of the devices based on the neat PFTSO2.

Conclusions

LEDs based on the PFO–PF3T and PFO–PFTSO2 blends show, in comparison to those based on neat PF3T or PFTSO2 copolymers, a remarkable increase of efficiency and luminance. Such improvements are attributed to a combination of spatial confinement of the excitons and to better charge transport and balance within the emissive layer. In addition, there is an efficient energy transfer process from PFO to the guest copolymers. We believe these blends provide all the benefits expected from the use of blends in LED fabrication.

Experimental

^1H and ^{13}C NMR spectra were recorded on a Varian spectrometer (300 MHz and 75 MHz, respectively) in $CDCl_3$ with tetramethylsilane as internal reference. FT-IR spectra were recorded using a Mattson 1000 spectrophotometer, dispersing the samples in KBr. Number-average ($\bar{M}_n$) and weight-average ($\bar{M}_w$) molecular weights were estimated by gel permeation chromatography (GPC) in a Waters 51 chromatograph equipped with two Waters UltraStyragel columns (1000 Å-500 Å) in series and with two detectors (a Water 410 Differential Refractometer and a Scanning Fluorescence Detector) at a flux rate of 1 ml min^{-1}. GPC analyses were performed on filtered solutions (0.45 μm, Millipore Millex HV) of the copolymers in tetrahydrofuran (THF) and using polystyrene standards.

UV/Vis absorption spectra of thin films deposited by spin coating on spectrosil discs were recorded with a Jasco V500 spectrophotometer. PL spectra were obtained on a Spex Fluorog F112A spectrofluorimeter. PEDOT–PSS, used as hole-injection material in LED fabrication, was provided by Bayer. After spin coating of the ITO with the PEDOT–PSS aqueous dispersion, these were left to dry under vacuum at about 100 °C for two hours. The polymer blends, containing 5% by weight of the guest copolymer, were spin coated from their mixed xylene solutions. Aluminium was thermally evaporated at a base pressure of 10^{-5} mbar, defining pixel areas of 4 mm^2. Ca cathodes were deposited inside a glove box at a pressure below 10^{-6} mbar and were protected with an overlayer of aluminium. LEDs were tested under vacuum (at about 10^{-2} mbar) and the EL spectra were recorded with an Oriel Instaspec IV CCD spectrograph.

Fluorescence decay curves were obtained by the single photon timing technique using picosecond laser excitation. A mode-locked Coherent Innova 400-1 argon ion laser synchronously pump a cavity-dumped Coherent 701-2 dye (DCM) laser, delivering 5–6 ps pulses with ~40 nJ $pulse^{-1}$ at a frequency of 460 kHz. The excitation light was generated by doubling the frequency of the output of the dye laser. The emission was selected by a Jobin-Yvon HR320 monochromator with a grating of 100 lines mm^{-1} and detected by a Hamamatsu 2809U-01 microchannel plate photomultiplier. The instrumental response function had an effective full width at half maximum (FWHM) of 35 ps. A total of about 20 000 counts were accumulated in the channel of maximum counts of the multichannel analyzer operating with 1024 channels.

Polymerization reactions

A more detailed description of the preparation procedure, particularly in the case of PFTSO2, is reported elsewhere.[28] The alternating copolymers were prepared using Suzuki coupling between the boron ester of 9,9-bis(2′-ethylhexyl)-fluorene and the appropriate dibrominated comonomer: 2,5-dibromothiophene *S*,*S*-dioxide,[29] in the case of PFTSO2, and 5,5″-dibromo-2,2′:5′2″-terthiophene, obtained according to reported procedures,[30,31] in the case of PF3T. The polymerization reactions were carried out in a refluxing THF–aqueous potassium carbonate (or sodium carbonate) (2 M) medium, in the presence of a catalytic amount of $Pd(PPh_3)_4$, for 3 to 7 days, in the dark and under N_2 and vigorous stirring. The copolymers were precipitated by dropwise addition of the cooled reaction mixture to methanol and collected by filtration. They were purified by dissolution in a minimum amount of

$CHCl_3$ and by the addition of the filtered solution to methanol. This procedure was repeated two more times. The collected copolymers were dried under vacuum for 24 hours.

Poly[9,9-bis(2′-ethylhexyl)fluorene-2,7-diyl-*alt*-(2,2′:5′2″-terthiophene-5,5″-diyl] (PF3T). PF3T was obtained as a bright orange powder in 47% yield. ^1H NMR: δ (ppm): 7.67–7.59 (6H, m, aromatic), 7.10–7.30 (6H, m, aromatic), 2.06 (4H, m, $-CH_2$), 0.55–0.88 (30 H, m, aliphatic). ^{13}C NMR: δ (ppm): 10.42, 14.03, 22.78, 27.21, 28.22, 33.91, 34.79, 44.47, 55.11, 120.17, 121.19, 123.74, 124.28, 124.71, 132.38, 133.69, 134.34, 136.12, 140.56, 144.23, 151.57. FT-IR (KBr, cm^{-1}): 3030, 2958, 2923, 2867, 1456, 1378, 818, 789. GPC: $\bar{M}_w = 4100$, $\bar{M}_n = 2800$, polydispersity 1.5.

Poly[9,9-bis(2′-ethylhexyl)fluorene-2,7-diyl-*alt*-*S*,*S*-dioxothiophene–2,5-diyl] (PFTSO2)[28]. PFTSO2 was isolated as an orange powder in 58% yield. ^1H NMR: δ (ppm): 7.84–7.64 (6H, m, aromatic), 7.11 (2H, s, thiophene), 2.11 (4H, m, $-CH_2$), 0.89–0.56 (30H, m, aliphatic). ^{13}C NMR: δ (ppm): 151.09, 150,08, 140.99, 127.44, 125.38, 124.58, 120.76, 119.26, 54.27, 43.40, 33.71, 32.84, 27.13, 26.00, 21.69, 12.99, 9.28. FT-IR (KBr, cm^{-1}): 2956, 2923, 2871, 1606, 1459, 1379, 1309 (SO_2), 1138 (SO_2), 890, 816. GPC: $\bar{M}_w = 27400$, $\bar{M}_n = 8700$, polydispersity 3.1.

References

1 J. J. M. Halls, J. Cornil, D. A. dos Santos, R. Silbey, D.-H. Hwang, A. B. Holmes, J.-L. Brédas and R. H. Friend, *Phys. Rev. B*, 1999, **60**, 5721.

2 J. J. M. Halls, C. A. Walsh, N. C. Greenham, E. A. Marseglia, R. H. Friend, S. C. Moratti and A. B. Holmes, *Nature*, 1995, **376**, 498.

3 G. Yu, J. Gao, J. C. Hummelen, F. Wudl and A. J. Heeger, *Science*, 1995, **270**, 1789.

4 M. Berggren, O. Inganäs, G. Gustafsson, J. Rasmusson, M. R. Andersson, T. Hjertberg and O. Wennerström, *Nature*, 1994, **372**, 444.

5 H. Vesteweber, R. Sander, A. Greiner, W. Heitz, R. F. Mahrt and H. Bässler, *Synth. Met.*, 1994, **64**, 141.

6 G. He, Y. Li, J. Liu and Y. Yang, *Appl. Phys. Lett.*, 2002, **80**, 4247.

7 R. Grupta, M. Stevenson, A. Dogariu, M. D. McGehee, J. Y. Park, V. Srdanov, A. J. Heeger and H. Wang, *Appl. Phys. Lett.*, 1998, **73**, 3492.

8 J. Liu, Y. Shi and Y. Yang, *Appl. Phys. Lett.*, 2001, **79**, 578.

9 H. Nishino, G. Yu, A. J. Heeger, T.-A. Chen and R. D. Rieke, *Synth. Met.*, 1995, **68**, 243.

10 G. He, J. Liu, Y. Li and Y. Yang, *Appl. Phys. Lett.*, 2002, **80**, 1891.

11 A. J. Campbell, D. D. C. Bradley and H. Antoniadis, *Appl. Phys. Lett.*, 2001, **79**, 2133.

12 X. L. Chen and S. A. Jenekhe, *Appl. Phys. Lett.*, 1997, **70**, 487.

13 X. Zhang, D. M. Kale and S. A. Jenekhe, *Macromolecules*, 2002, **35**, 382.

14 I.-N. Kang, D.-H. Hwang, H.-K. Shim, T. Zyung and J.-J. Kim, *Macromolecules*, 1996, **29**, 165.

15 Y. C. Kim, T. W. Lee, O. O. Park, C. Y. Kim and H. N. Cho, *Adv. Mater.*, 2001, **13**, 646.

16 C. I. Wilkinson, D. G. Lidzey, L. C. Palilis, R. B. Fletcher, S. J. Martin, X. H. Wang and D. D. C. Bradley, *Appl. Phys. Lett.*, 2001, **79**, 171.

17 J. Morgado, R. H. Friend and F. Cacialli, *Appl. Phys. Lett.*, 2002, **80**, 2436.

18 J. Morgado, E. Moons, R. H. Friend and F. Cacialli, *Adv. Mater.*, 2001, **13**, 810.

19 M. Wohlgenannt, W. Graupner, F. P. Wenzl, S. Tasch, E. J. W. List, G. Liesing, M. Graupner, A. Hermetter, U. Rohr, P. Schlichting, Y. Geerts, U. Scherf and K. Müllen, *Chem. Phys.*, 1998, **227**, 99.

20 A. Montalli, G. S. Harms, A. Renn, C. Weder, P. Smith and U. P. Wild, *Phys. Chem. Chem. Phys.*, 1999, **1**, 5697.

21 H. N. Cho, J. K. Kim, D. Y. Kim, C. Y. Kim, N. W. Song and D. Kim, *Macromolecules*, 1999, **32**, 1476.

22 A. R. Buckley, M. D. Rahn, J. Hill, J. Cabanillas-Gonzalez, A. M. Fox and D. D. C. Bradley, *Chem. Phys. Lett.*, 2001, **339**, 331.

23 A. Charas, J. Morgado, J. M. G. Martinho, L. Alcácer and F. Cacialli, *Chem. Commun.*, 2001, 1216.

24 A. J. Campbell, D. D. C. Bradley and H. Antoniadis, *J. Appl. Phys.*, 2001, **89**, 3343.

25 A. Charas, J. Morgado, J. M. G. Martinho, L. Alcácer and F. Cacialli, *Synth. Met.*, 2002, **127**, 251.

26 T. M. Brown, J. S. Kim, R. H. Friend, F. Cacialli, R. Daik and W. J. Feast, *Appl. Phys. Lett.*, 1999, **75**, 1679.

27 M. Redecker, D. D. C. Bradley, M. Inbasekaran and E. P. Woo, *Appl. Phys. Lett.*, 1998, **73**, 1565.

28 A. Charas, J. Morgado, J. M. G. Martinho, L. Alcácer, S. F. Lim, R. H. Friend and F. Cacialli, submitted for publication in *Polymer*.

29 N. Furukawa, H. Hoshiai, T. Shibutani, M. Higaki, F. Iwasaki and H. Fujihara, *Heterocycles*, 1992, **34**, 1085.

30 P. A. Chaloner, S. R. Gunutunga and P. B. Hitchcock, *J. Chem. Soc., Perkin Trans. 2*, 1997, 1597.

31 P. Bäuerle, F. Würthner, G. Götz and F. Effenberger, *Synthesis*, 1993, 1099.